Journal of the Argentine Chemical Society

URANIUM (VI) AND ZIRCONIUM (IV) OF THE SECOND-GENERATION QUINOLONE ANTIMICROBIAL DRUG NORFLOXACIN: STRUCTURE AND BIOLOGICAL ACTIVITY

Sadeek A. Sadeek[1♥], Akram M. El-Did Amony[1], Walaa H. El-Shwiniy[1], and Wael A. Zordok[1]

[1]*Department of Chemistry, Faculty of Science, Zagazig University, Zagazig, Egypt.*

Received March 16, 2010. In final form August 10, 2010.

Abstract

Two new norfloxacin complexes were prepared from the interaction of Zr(IV) and U(VI) with norfloxacin (NOR) in methanol and acetone, at room temperature and separated as solids with characteristic colors. Elemental analysis, infrared and UV-Vis spectroscopy, conductance measurements, ^{1}HNMR and thermal analyses have been used to characterize the isolated solid complexes. The results support the formation of the complexes with the formula $[ZrO(NOR)_2Cl]Cl.15H_2O$ and $[UO_2(NOR)_3](NO_3)_2.4H_2O$. The infrared spectra of the isolated solid complexes suggested that the norfloxacin react as bidentate ligand through the carbonyl oxygen atom and one oxygen atom of the carboxylic group forming six atoms rings with the metal ions. The bond stretching force constant and length of the U=O bond for the $[UO_2(NOR)_3](NO_3)_2.4H_2O$ complex were

♥Corresponding author. E mail: sadeek59@yahoo.com

calculated. The interpretation, mathematical analysis and evaluation of kinetic parameters of thermogravimetric (TGA) results and its differential (DrTGA), such as entropy of activation, pre-exponential factors, and activation energy evaluated by using Coats-Redfern and Horowitz-Metzger equations for the two complexes were carried out. General mechanisms describing the decomposition of the solid complexes are suggested. The exact structure of Zr(IV) complex was detected by using the density functional theory (DFT) at the B3LYP/CEP-31G level of theory. Antimicrobial studies were carried out using agar diffusion method against several bacterial species, such as *Staphylococcus aureus* (*S. aureus*), E*scherichia coli* (*E. coli*) and *Pseudomonas aeruginosa* (*P. aeruginosa)* and antifungal screening was studied against two fungi species, *penicillium* (*P. rotatum*) and t*richoderm*a (*T. sp*.). The results showed significant increase in antibacterial activity of metal complexes as compared with uncomplexed ligand and no antifungal activity observed for ligand and their complexes. This increase in the activity is being considered due to increased bioavailability of the metal drug complexes and the aqueous solubility of norfloxacn.
Keywords: norfloxacin; DFT; ^{1}HNMR; microbial activity; thermal analysis

Resumen
Dos nuevos complejos de norfloxacina fueron preparados a temperatura ambiente y separados como sólidos con colores característicos, a partir de la interacción de Zr(IV) y U(VI) con norfloxacina (NOR) en metanol y acetona, Análisis elemental, espectroscopías infrarroja y UV-VIS, mediciones de conductancia, 1HNMR y análisis térmico se utilizaron para caracterizar los complejos sólidos aislados. Los resultados apoyan la formación de los complejos con la fórmula $[ZrO(NOR)_2Cl]Cl.15H_2O$ y $[UO_2(NOR)_3](NO_3)_2.4H_2O$. El espectro infrarrojo de los complejos sugirió que la norfloxacina reacciona como ligando bidentado a través del átomo de oxígeno carbonílico y un átomo de oxígeno del grupo carboxílico formando anillos de seis átomos con los iones metálicos. Se calcularon la constante de fuerza del estiramiento y la longitud del enlace U = O en el complejo $[UO_2(NOR)_3](NO_3)2.4H_2O$. Se llevó a cabo además la interpretación, el análisis matemático y la evaluación de parámetros cinéticos de los resultados termogravimétricos (TGA) y su diferencial (DrTGA), tales como la entropía de la activación, factores pre-exponential y la energía de activación los que fueron evaluados mediante el uso de ecuaciones de Coats-Redfern y Horowitz-Metzger para los dos complejos. Se proponen mecanismos generales que describen la descomposición de los complejos sólidos. La estructura exacta del complejo Zr(IV) se propone mediante el uso de la teoría del funcional de densidad (DFT) en el nivel teórico B3LYP/CEP-31 G. Estudios antimicrobianos se llevaron a cabo utilizando el método de difusión de agar frente a varias especies bacterianas, tales como *Staphylococcus aureus* (*S. aureus*), *Escherichia coli* (*e. coli*) y *Pseudomonas aeruginosa* (*p. aeruginosa*), mientras que el cribado antimicótico fue estudiado contra las especies de hongos, *penicillium* (*p. rotatum*) y *trichoderma* (*T. sp*.). Los resultados mostraron un incremento significativo en la actividad antibacteriana de los complejos metálicos, en comparación con el ligando sin complejar y ninguna actividad antimicótica fue observada para el ligando y sus complejos.
Palabras clave; norfloxacina; DFT; ^{1}HNMR; actividad antimicrobiana; análisis térmico

Introduction

Quinolones are active against a wide range of gram-positive cocci and gram-negative organisms [1]. Bacterial DNA exists in a supercoiled form and the enzyme DNA gyrase, a topoisomerase, is responsible for introducing negative supercoils into the structure. Quinolone antibacterial drugs act by inhibiting the activity of the bacterial DNA gyrase, preventing the normal functioning of DNA. Nalidixic acid is the first member of quinolone carboxylic acid family of antimicrobials introduced into clinical practice which used in the treatment of urinary tract infections [2]. A major advanced in activity occurred with the introduction of fluorine atom on position six into the quinoline ring to enhance the spectrum and the potency of activity, and with addition of piperazinyl group on position seven to enhance permeability and potency [3].

The synthesis and characterization of new metal complexes with quinolone antibacterial agents are of great importance for understanding the drug-metal ion interaction and for their potential pharmacological use. Low solubility of quinolones and their complexes in pH region 5 to 10 represents a great difficulty in preparing single crystals of quinolone metal complexes. A few

crystal structures where quinolone is coordinated to the metal ion are known [4-8]. On the other side, numerous crystal structures of mixed metal complexes with coordinated quinolones and N-, S- or O-donors have been reported [9-15]. Norfloxacin is a member of the fluoroquinolone class of synthetic antimicrobial agents with the widest clinical use and present in the zwitterionic state (Formula I), which is active against various Gram-positive as well as Gram-negative microorganisms. The complexation of norfloxacin with metal cations increasing the solubility of norfloxacin. The increase in the aqueous solubility of norfloxacin can have profound effect on the enteric absorption of norfloxacin and on its antibacterial activity when these metal cations are present. Density Functional Theory (DFT) was used to compute the cation type influence on theoretical parameters and detect the exact structure of the Zr(IV) compound. Such computational characterization reduces time consuming experiments for biomedical and pharmaceutical studies of the drugs and its complexes. Profiles of the optimal set and geometry of these complexes were simulated by applying the GAUSSIAN 98W package of programs [16] at B3LYP/CEP-31G [17] level of theory.

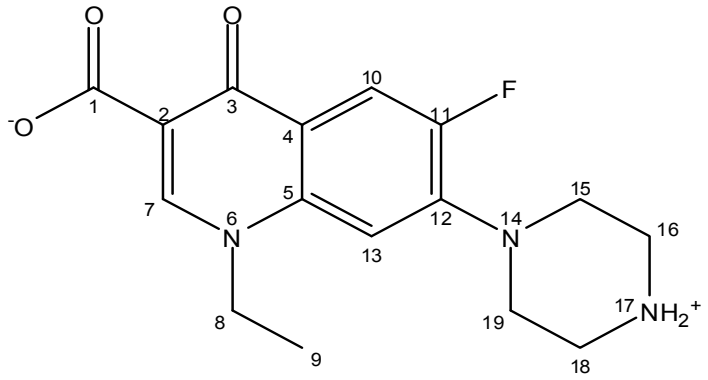

Formula I. Structure of norfloxacin (NOR) and its zwitterionic structure.

The aim of the present work is to investigate the new solid norfloxacin complexes formed from the reaction of zirconyl chloride and dioxouranium nitrate with norfloxacin in methanol and acetone as a solvent using infrared spectra, electronic reflection, thermogravimetric analysis, ^{1}HNMR and Density Function Theory (DFT).

Experimental

Chemicals

Norfloxacin used in this study was obtained from the Egyptian International Pharmaceutical Industrial Company (EIPICO). All chemicals used for the preparation of the two complexes were of analytical reagent grade, commercially available from different sources. $ZrOCl_2.8H_2O$ (99.9%, Fluka Co.), $UO_2(NO_3)_2.6H_2O$ (99.9%, Aldrich Co.) were used without further purification.

Synthesis

The orange solid complex $[ZrO(NOR)_2Cl]Cl.15H_2O$ was prepared by adding 0.5mmol (0.1610g) of zirconyl chloride ($ZrOCl_2.8H_2O$) in 10ml bidistilled water drop wisely to a stirred suspended solution of 1mmol (0.3193g) of NOR in 50ml methanol. The reaction mixture was stirred for 15h at 35 ^{o}C. The orange precipitate was filtered off and dried *in vacuo* over $CaCl_2$. The

pale yellow solid complex $[UO_2(NOR)_3](NO_3)_2.4H_2O$ was prepared in a similar manner described above by using acetone instead of methanol and using $UO_2(NO_3)_2.6H_2O$ in 1:3 molar ratio. Qualitative black ring test for ionic nitrate using freshly prepared $FeSO_4$ solution and concentrated sulfuric acid, a black ring of $FeSO_4.NO$ is formed led to the presence of nitrate as counter ions in the uranyl/NOR complex and for the other complex the qualitative reactions revealed the presence of chloride as counter ions. The percentage of chloride ions was estimated volumetrically with an aqueous solution of $AgNO_3$ according to the known method [18]. The two complexes were characterized by their elemental analysis, infrared, electronic, ^{1}HNMR and thermal analysis.

Instruments

Elemental C, H, N and halogen analysis were carried out on a Perkin Elmer CHN 2400. The percentage of the metal ions was determined gravimetrically by transforming the solid products into oxide, and also determined by using atomic absorption method. Spectrometer model PYE-UNICAM SP 1900 fitted with the corresponding lamp was used for this purposed. IR spectra were recorded on FTIR 460 PLUS (KBr discs) in the range from 4000-400 cm^{-1}, ^{1}HNMR spectra were recorded on Varian Mercury VX-300 NMR Spectrometer using DMSO-d_6 as solvent. TGA-DrTGA measurements were carried out under N_2 atmosphere within the temperature range from room temperature to 800 ^oC using TGA-50H Shimadzu. Electronic spectra were obtained using UV-3101PC Shimadzu with a 1cm quartz cell. Molar conductivities in DMSO at 1.0×10^{-3} M were measured on CONSORT K410.

Antibacterial investigation

Antibacterial activity of the complexes/ligand was investigated by a previously reported modified method of Beecher and Wong [19], against different bacterial species, such as *Staphylococcus aureus (S. aureus), Escherichia coli (E. coli)* and *Pseudomonas aeruginosa (P. aeruginosa)*. The microorganisms were purchased from the laboratory of (Chemical Biology) in the Faculty of Science, Zagazig University. The nutrient agar medium (0.5% Peptone, 0.1% Beef extract, 0.2% Yeast extract, 0.5% NaCl and 1.5% Agar-Agar) was prepared and then cooled to 47 ^oC and seeded with tested microorganisms. After solidification 5mm diameter holes were punched by a sterile Cork-borer. The investigated compounds, ligand and their complexes, were introduced in Petri-dishes (only 0.1ml) after dissolving in DMSO. The plates were then incubated for 20 h at 37 ^oC. At the end of incubation period the inhibition zone around each hole was measured.

Results and discussion

The analytical data and physical properties of the coordination compounds are listed in Table 1. The ligand coordinate to Zr(IV) and U(VI) ions in a 1:2 and 1:3 molar ratio which was established from the results of the chemical analysis (Table 1) and also the two prepared complexes contain water molecules. The number of bound water molecules in these compounds being different. The IR spectroscopic and thermogravimetric data also confirm water in the composition of the complexes. All compounds are stable in air and the melting points of the complexes are higher than that of the ligand revealing that the complexes are much more stable than ligand.The molar conductance values of the free norfloxacin , Zr(IV) and U(VI) norfloxacin complexes were found at 25 ^oC (Table 1), which indicates that the complexes are of higher electrolytic nature than ligand [20]. The low conductivity values are in agreement with the low solubility of NOR complexes in water, ethanol, chloroform, acetone and most organic solvents. On the other hand, they are soluble in DMSO, DMF and concentrated acids. Qualitative reactions revealed the presence of chloride and nitrate ions in the Zr(IV) and U(VI) complexes as counter ions.

Table 1. Physico-analytical data oflignorfloxacin and its metal complexes.

Complexes M.Wt. (M.F.)	Yield%	mp/°C	color	Content (calculated) found					Λ (S cm^2 mol^{-1}) (Ω^{-1}cm^2 mol^{-1})
				% C	% H	% N	% M	% Cl	
NOR	-	230	Buff	(60.13)	(5.64)	(13.15)	-	-	-16.64
319.331 ($C_{16}H_{18}N_3O_3F$)				60.11	5.64	13.14			
$[ZrO(NOR)_2Cl]Cl.15H_2O$	93.90	260	orange	(35.35)	(6.08)	(7.73)	(8.40)	(6.54)	252.72
1086.2 ($C_{32}H_{66}N_6O_{22}O_{l2}F_2Cl_2Zr$)				35.15	6.07	7.46	8.33	6.54	
$[UO_2(NOR)_3](NO_3)_2.4H_2O$	69.38	300	Pale	(40.48)	(4.36)	(10.82)	(16.73)	-	34.32
1423 ($C_{48}H_{62}N_{11}O_{21}F_3U$)			yellow	40.94	4.91	10.82	16.70		

IR data and bonding

The assignments of IR bands (Figure 1 and Table 2) were made by comparing the spectra of the complexes with those of free ligand in order to determine the site of coordination that may be involved in chelation. The presence of a broad water bands at 3412 and 3424 cm^{-1} confirms the presence of water molecules in the two prepared complexes and also a group of weak and medium intensity bands around 2928 and 2480 cm^{-1} which assigned to the vibration of the quaternized nitrogen of the piperazinyl group indicates that the zwitterionic form of NOR is involved in the coordination to the metal ions investigated [21-29,38].

The infrared spectrum of free norfloxacin exhibits a very strong bands at 1729 and 1619 cm^{-1}, Table 2, which are assigned to the stretching vibration of the carboxylic ν(COOH) and the pyridone stretch *ν*(C=O) [21-25]. These bands disappear in the complexes which indicative of the involvement of the carboxylic group and the carbonyl oxygen atom in the interaction with metal ions. The spectra of our two complexes also show two medium strong bands at 1385 and 1382 cm^{-1}. These bands are absent in the spectrum of NOR and most likely due to the symmetric vibration of ligated COO^- group [24-31].

The carboxylato group can act as unidentate, bidentate or as bridging ligand and the frequency separation [$\Delta\nu=\nu_{as}(COO^-)-\nu_s(COO^-)$] between the asymmetric and symmetric stretching of this group [32,33] can be made to distinction between these binding states. Deacon and Phillips [33] investigate the asymmetric and symmetric stretching vibrations of large number of carboxylato complexes with known crystal structure, they found that for unidentate carboxylate complexes exhibit $\Delta\nu$ values which are much larger than those of the ionic salts ($\Delta\nu$ > 200 cm^{-1}). The observed $\Delta\nu$ for our investigated solid complexes Zr(IV) and U(VI) are 243 cm^{-1} and 249 cm^{-1}, which suggest a unidentate interaction of the carboxylate group. However, the C, H and N elemental analysis of the complexes reported in this work are different from the values reported for the isolated dimeric complex [34], which indicate that these complexes are, most probably, monomeric.

New bands are found in the spectra of the complexes at 566, 512 cm^{-1} for Zr(IV) and at 565, 513 cm^{-1} for U(VI), which are assigned to ν(M-O) stretching vibrations of coordinated carboxylato oxygen atom and carbonyl oxygen atom. According to the above discussion the NOR is coordinated to metal ions as a bidentate ligand through the oxygen atom of the carboxylato group and the oxygen atom of the carbonyl group.

Table 2. Infrared frequencies[a](cm^{-1}) and tentative assignments[b] for (A) Norfloxacin (NOR); (B) $[ZrO(NOR)_2Cl]Cl.15H_2O$, (C) $[UO_2(NOR)_3](NO_3)_2.4H_2O$.

A	B	C	Assignment
3425w	3412m,br	3424m,br	ν(O-H); H_2O , COOH
3332vw	-	-	ν(N-H)
3046ms	2971vw,sh	3066w	ν(C-H)
2828vw	-	2853w	$\nu(-NH_2^+)$
2728m	-	2676vw	
2554ms	2480vw	2476vw	
1729vs	-	-	ν(C=O);COOH
-	1628vs,sh	1631vs	$\nu_{as}(COO^-)$
1619vs	1590vw	1580sh	ν(C=O) and phenyl breathing modes
1586vs	1524vw	1550vw	
1521w		1500sh	
1479s	1482vs	1472vs	-CH; deformations of
1443w			$-CH_2$
1406vw			
-	1385ms	1382s,sh	$\nu_s(COO^-)$
1376ms	-	1271s	$\delta_b(-CH_2)$
1303vw			
1250vs	1270vs	1206vw	ν(C-C),
1204w	1190s	1145m	ν(C-O),
1143vw	1139vs,sh	1092w	ν(C-N)
1124vw	1087m	1038ms	$\delta_r(-CH_2)$
1097s	1035ms		
1030ms			
937vs,sh	974vw	983w	-CH bend; phenyl
885ms	933ms		
833s	896w	854vw	
-		904vs,sh	ν_{as}(U=O)
		818s	ν_s(U=O)
	811ms,sh		ν(Zr=O)
798vw	751ms	784vw	$\delta_b(COO^-)$
782w		747s	
747ms		702w	
700m			
660w	626vw,sh	664vw	ν(M-O) ring+deformation
621m	566w	628m	
561m	512m	565m	
516vw		513vw	
505vw		480m	
449m			

[a]s = strong, w = weak, sh = shoulder, v =very, br = broad, [b]ν = stretching, δ = bending.

For $[UO_2(NOR)_3](NO_3)_2.4H_2O$ complex, the most probably structure is shown in Formula II, where the six oxygen atoms of their NOR ligands occupy equatorial positions around the central metal atom U(VI), forming a plane containing the six-membered rings and the two oxygen atoms of the uranyl group occupy axial positions. The complex possesses one plane of symmetry and no axes of symmetry therefore may have C_s symmetry and are expected to display 372 vibrational fundamentals which are all monodegenerate. These are distributed between motions of the type $A^{\backslash}$ and $A^{\backslash\backslash}$; all are infrared active. The four vibrations of the UO_2 unit in the complex are of the type $3A^{\backslash}$ and $A^{\backslash\backslash}$, these are ν_s(U=O)**,** $A^{\backslash}$; ν_{as}(U=O)**,** $A^{\backslash}$; $\delta(UO_2)$**,** $A^{\backslash}$ and $\delta(UO_2)$, $A^{\backslash\backslash}$. The data given in

Table 2 show that the v_{as}(U=O) absorption band of this complex occurs as a very strong singlet at 904 cm^{-1} and the v_s(U=O) absorption band occur at 818 cm^{-1}. These assignments for the stretching vibrations of the uranyl group, UO_2, agree quite well with those known for many dioxouranium (VI) complexes [35-37] .The v_s(U=O) value was used to calculate both the bond length and force constant, F(U=O), for the UO_2 bond in our complex according to the known method [35,36] . The calculated bond length and force constant values are 1.749 Å and 647.35 Nm^{-1}.

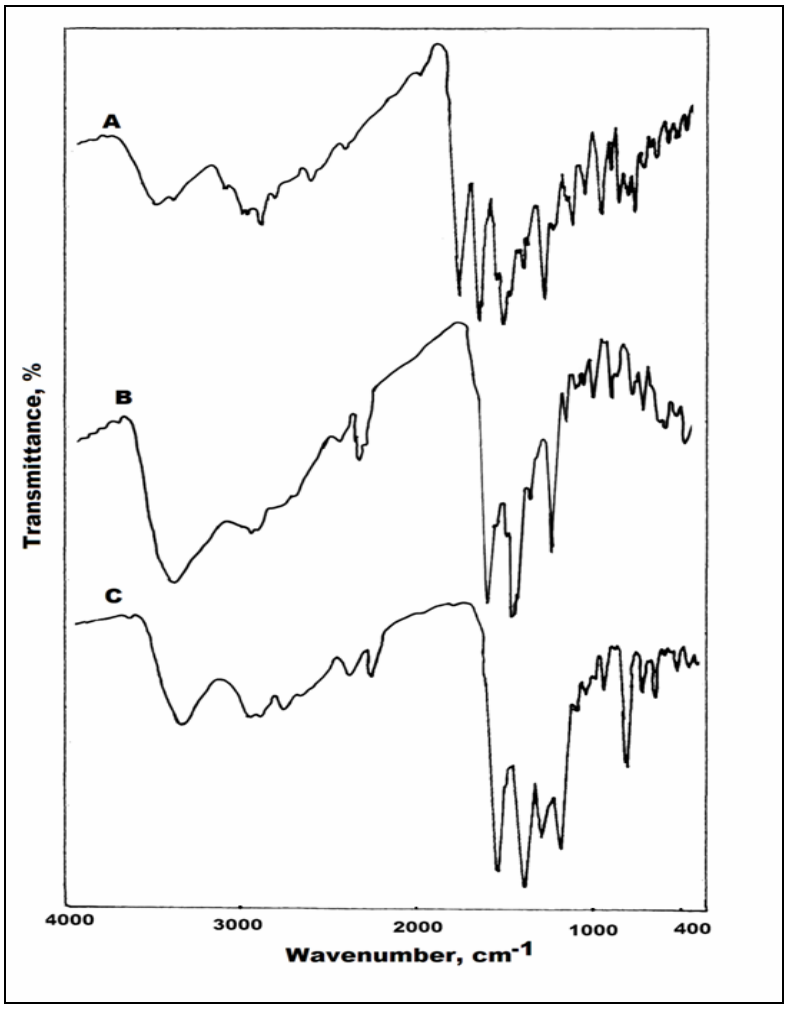

Figure 1. Infrared spectra of (A) Norfloxacin (NOR); (B) $[ZrO(NOR)_2Cl]Cl.15H_2O$ and (C) $[UO_2(NOR)_3](NO_3)_2.4H_2O$.

UV-Vis. Spectra

The electronic solid reflection spectra of the norfloxacin along with the Zr(IV) and U(VI) complexes are shown in Figure 2. The free norfloxacin reflected at 252, 316 and 355 nm which attributed to π-π^* and n-π^* intraligand transitions (these transitions occur in case of unsaturated hydrocarbons which contain ketone groups) [38]. The reflection spectra for Zr(IV) and U(VI) norfloxacins show two bands for each complex which were found at 281, 323 nm and 291, 298 nm, respectively, the shift of the reflectance λ_{max} to lower values (*hypsochromic shift*) for two complexes and the absent of reflection band at 252 nm in our two mentioned complexes attributed to

complexation behavior of norfloxacin towards metal ions. The two complexes have a band at ~ 360 nm which may be assigned to the ligand to metal charge-transfer [39,40].

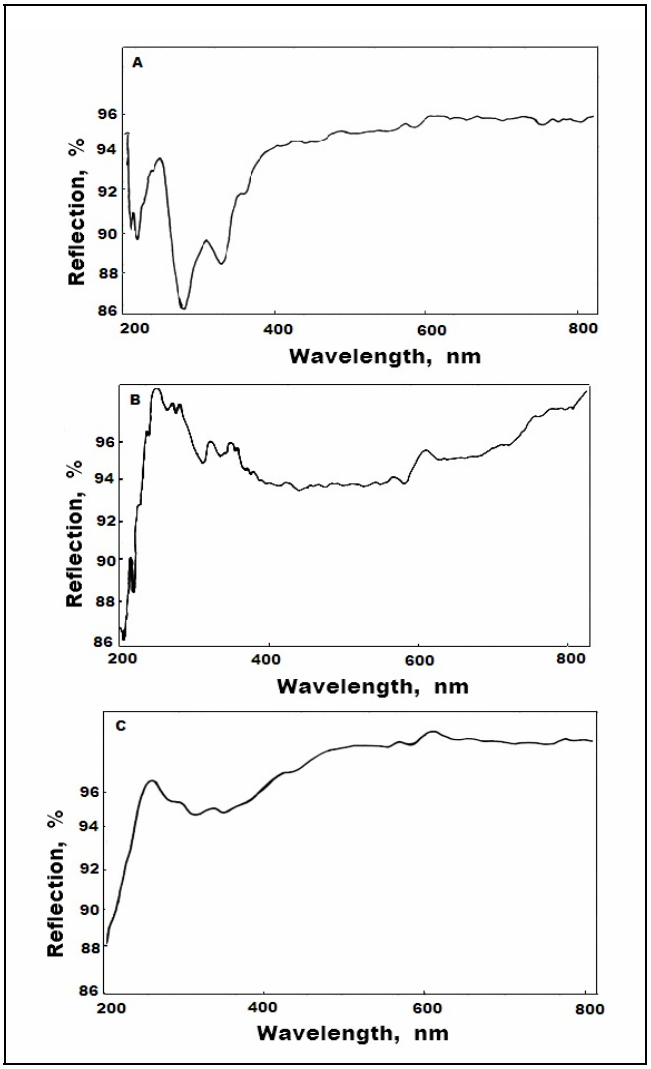

Figure 2. Electronic reflection spectra of (A): NOR; (B) $[ZrO(NOR)_2Cl]Cl.15H_2O$ and (C) $[UO_2(NOR)_3](NO_3)_2.4H_2O$.

Thermal analyses

Thermal stabilities of norfloxacin, $[ZrO(NOR)_2Cl]Cl.15H_2O$ and $[UO_2(NOR)_3](NO_3)_2.4H_2O$ were studied using thermogravimetric (TG) and differential thermogravimetric (DrTG) analyses from ambient temperature to 800 ^oC under N_2 flow, Figure 3. The temperature ranges and percentage mass losses of the decomposition reaction are given in Table 3, together with evolved moiety and theoretical percentage mass losses. The data obtained indicate that the norfloxacin is thermally stable in the temperature range 25-56 ^oC. Decomposition of the NOR start at 59 ^oC and finished at 726 ^oC with two stages. The first stage of decomposition occurs at maximum temperature of 116 ^oC and is accompanied by a weight loss of 8.75%. The second stage of decomposition occurs at three maxima 330, 423 and 654 ^oC and is accompanied by a weight loss of

83.73%. The actual weight loss from these stages is equal to 92.48%, very closer to calculated value 92.46%.

The thermal decomposition of $[ZrO(NOR)_2Cl]Cl.15H_2O$ complex in inert atmosphere proceeds approximately with two main degradation steps. The step of decomposition occurs at maximum temperature of 55 ^oC and is accompanied by weight loss of 9.91%, corresponding to the loss of six water molecules. The second stage of decomposition occurs at maximum temperature of 398 and 605 ^oC. The weight loss of this step is 62.147% and the final product obtained at 800 ^oC is ZrO_2.

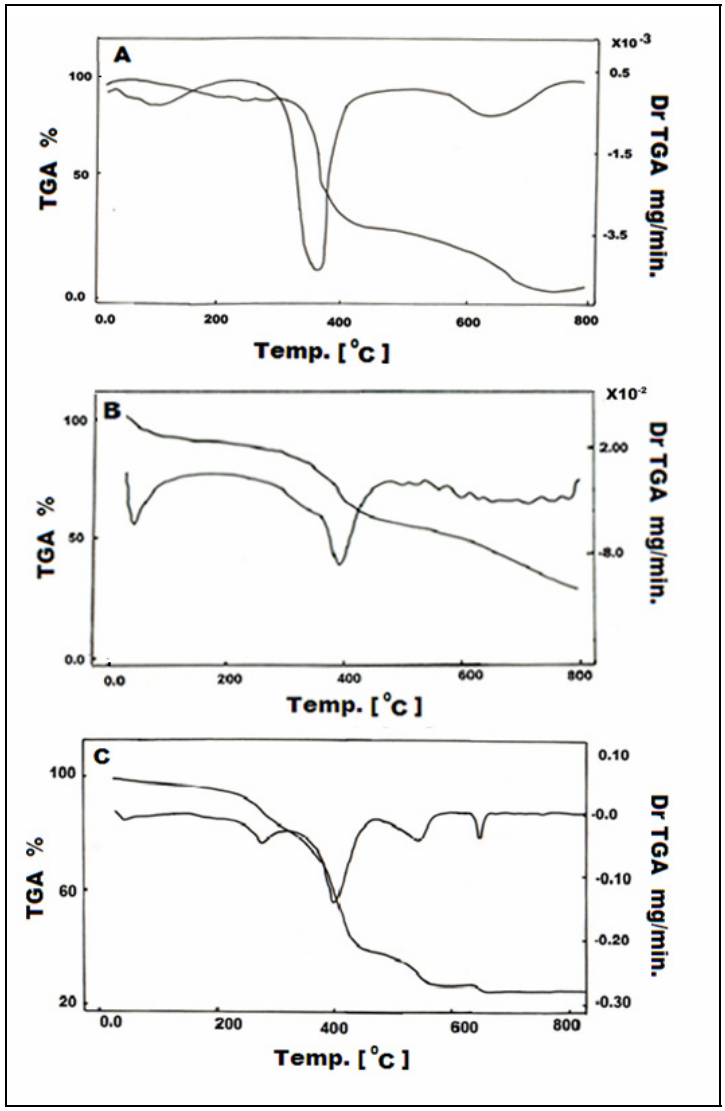

Figure 3. TGA and DTG diagrams of (A): NOR; (B) $[ZrO(NOR)_2Cl]Cl.15H_2O$ and (C) $[UO_2(NOR)_3](NO_3)_2.4H_2O$.

Hydrated U(VI) norfloxacin complex loss upon heating rate four water molecules in the first stage at maximum temperature 58 ^oC (Table 3). The second step of decomposition occurs at four maxima temperature 280, 399, 543 and 646 ^oC. This step is associated with the loss of norfloxacin forming UO_2 as a final product.

The final products of two complexes obtained at 800 ^{o}C are characterized by the infrared spectra which show the characteristic spectrum for metal oxides and the absence of all bands associated with the norfloxacinate group.

The proposed structure formula on the basis of the results discussed in this paper located as shown in formula II:

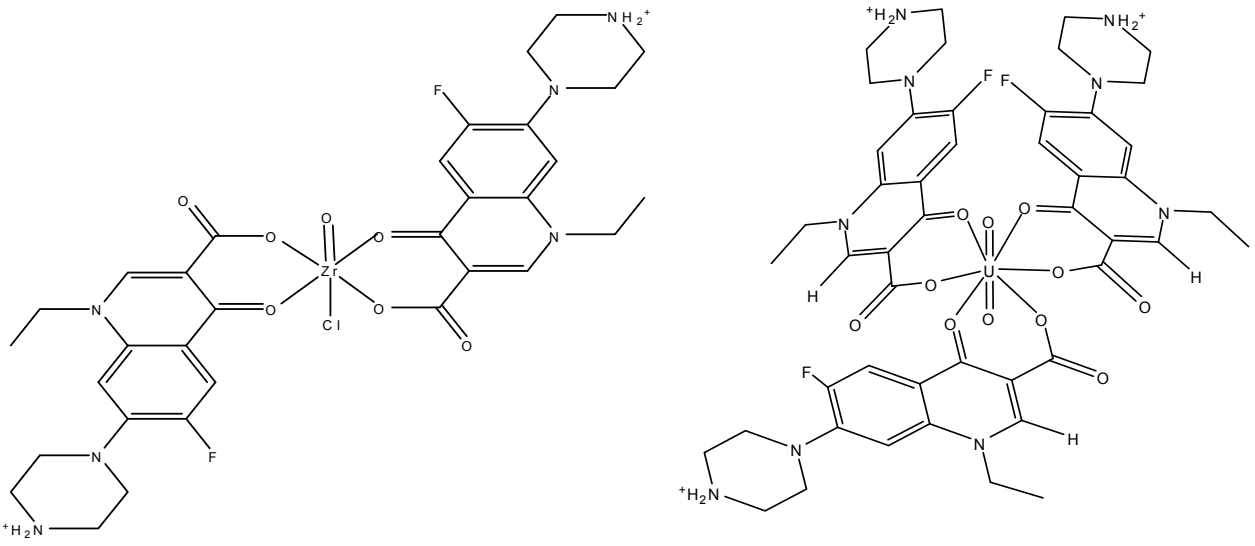

Formula II. The coordination mode of Zr(IV) and U(VI) with norfloxacin

Table 3. The maximum temperature T_{max} (^{o}C) and weight loss values of the decomposition stages for Zr(IV) and U(VI) norfloxacins.

Compounds	Decomposition	Tmax/^{o}C	Weight loss (%)	
			Calc.	Found
NOR	First step	116	8.77	8.75
($C_{16}H_{18}N_3O_3F$)	Second step	330, 423, 654	83.69	83.73
	Total loss, Residue		92.46, 7.54	92.48, 7.52
$[ZrO(NOR)_2Cl]Cl.15H_2O$	First step	55	9.94	9.91
($C_{32}H_{66}N_6O_{22}F_2Cl_2Zr$)	Second step	398, 605	62.142	62.147
	Total loss, Residue		72.082, 27.918	72.057, 27.947
$[UO_2(NOR)_3](NO_3)_2.4H_2O$	First step	58	5.06	5.16
($C_{48}H_{62}N_{11}O_{21}F_3U$)	Second step	280, 399, 543, 646	70.91	70.73
	Total loss, Residue		75.97, 24.03	75.89, 24.11

The kinetic studies

There has been increasing interest in determining rate-dependent parameters of solid-state non-isothermal decomposition reactions by analysis of TG curves. Several equations have been proposed to analyze a TG curve and obtain values for kinetic parameters [41-48].

In the present investigation the general thermal behavior of the norfloxacin ligand and the two complexes in terms of stability ranges, peak temperatures and values of kinetic parameters, are shown in Figure 4 and Table 4. The kinetic parameters have been evaluated using the following methods and the results obtained by these methods are compared with one another. The following two methods are briefly discussed.

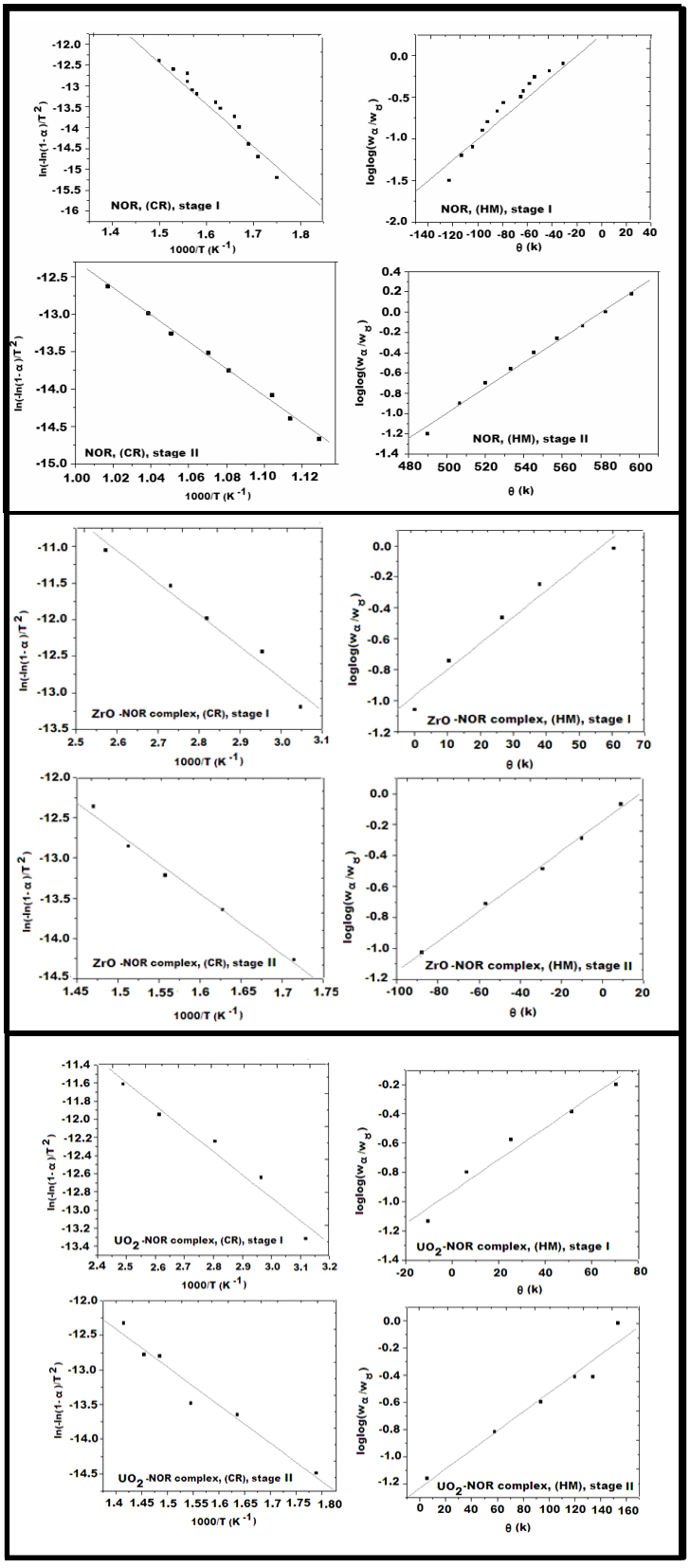

Figure 4. The diagrams of kinetic parameters of norfloxacin, $[ZrO(NOR)_2Cl]Cl.15H_2O$, and $[UO_2(NOR)_3](NO_3)_2.4H_2O$ complexes using Coats-Redfern (CR) and Horowitz-Metzger (HM) equations**.**

Table 4. Thermal behavior and kinetic parameters determined using the Coats–Redfern (CR) and Horowitz–Metzger (HM) operated for norfloxacin and their complexes.

Complexes	Decomposition Range (K)	T_s (K)	Method	Parameter					R^a	SD^b
				$E^*\times10^4$ (J mol^{-1})	$A\times10^3$ (s^{-1})	$\Delta S^*\times10^2$ (J mol^{-1} K^{-1})	$\Delta H^*\times10^4$(J mol^{-1})	$\Delta G^*\times10^5$ (J mol$^{-1)}$		
NOR	537-734	696	CR	8.295	5.944×10^2	-1.958	7.716	2.135	0.9216	0.31
			HM	11.585	6.838×10^4	-1.020	11.006	1.810	0.8661	0.20
	844-996	927	CR	17.5	16.7	-1.74	16.7	3.28	0.9945	0.19
			HM	19.1	3.82×10^5	-0.9	18.3	2.67	0.9948	0.09
$[ZrO(NOR)_2Cl]Cl.15H_2O$	328	328	CR	3.638	2.839×10	-1.605	3.365	0.8628	0.9707	0.16
($C_{32}H_{66}N_6O_{22}F_2Cl_2Zr$)			HM	3.494	1.482	-1.850	3.221	0.9289	0.9631	0.09
	671	671	CR	6.253	8.655	-1.763	5.695	1.753	0.9880	0.09
			HM	8.388	3.581×10^2	-1.453	7.830	1.758	0.9968	0.02
$[UO_2(NOR)_3](NO_3)_2.4H_2O$	331	331	CR	2.114	0.0638	-2.112	1.839	0.8831	0.9640	0.15
($C_{48}H_{62}N_{11}O_{21}F_3U$)			HM	2.282	0.4727	-1.946	2.007	0.8448	0.9621	0.08
	553	553	CR	4.583	0.240	-2.045	4.123	1.543	0.9600	0.17
			HM	4.093	0.560	-1.974	3.633	1.455	0.9520	0.09

a=correlation coefficients of the Arrhenius plots and b=standard deviation.

Coats-Redfern equation

The Coats-Redfern equation (1), which is a typical integral method, can be represented as:

$$\int_0^{\alpha} \frac{d\alpha}{(1-\alpha)^n} = \frac{A}{\varphi}\int_{T1}^{T2} \exp\left(\frac{-E^*}{RT}\right) dT \qquad (1)$$

For convenience of integration, the lower limit T_1 is usually taken as zero. This equation on integration gives:

$$\ln\left[\frac{-\ln(1-\alpha)}{T^2}\right] = \frac{-E^*}{RT} + \ln\left[\frac{AR}{\varphi E^*}\right] \qquad (2)$$

Aplot of left-hand side (LHS) against $1/T$ was drawn. E* is the energy of activation in k J mol^{-1} and calculated from the slope and A in (s^{-1}) from the intercept. The entropy of activation ΔS* in (J $K^{-1}mol^{-1}$) was calculated by using equation (3):

$$\Delta S^* = R \ln\left(\frac{Ah}{K_B T_s}\right) \qquad (3)$$

Where k_B is the Boltzmann constant, h is the Plank's constant and T_s is the DTG peak temperature [49].

Horowitz-Metzger equation

The Horowitz-Metzger equation is an illustrative of the approximation methods. These authors derived the relation:

$$\log\left[\frac{\{1-(1-\alpha)^{1-n}\}}{(1-n)}\right] = \frac{E^*\theta}{2.303RT_s^2} \quad \text{for } n \neq 1 \qquad (4)$$

When n = 1, the LHS of equation 8 would be log[-log (1-α)]. For a first-order kinetic process the *Horowitz-Metzger* equation may be written in the form:

$$\log\left[\log\left(\frac{w_\alpha}{w_\gamma}\right)\right] = \frac{E^*\theta}{2.303RT_s^2} - \log 2.303 \qquad (5)$$

Where $\theta = T - T_s$, $w_\gamma = w_\alpha - w$, w_α = mass loss at the completion of the reaction; w = mass loss up to time t. The plot of log[log(w_α / w_γ)] versus θ was drawn and found to be linear from the slope of which E^* was calculated. The pre-exponential factor, A, was calculated from the equation:

$$\frac{E^*\theta}{RT_s^2} = \frac{A}{\left[\varphi \exp\left(-\frac{E^*}{RT_s}\right)\right]} \qquad (6)$$

The entropy of activation, ΔS^*, was calculated from equation (3). The enthalpy of activation, ΔH^*, and Gibbs free energy, ΔG^*, were calculated from;

$$\Delta H^* = E^* - RT \qquad (7)$$

and

$$\Delta G^* = \Delta H^* - T\Delta S^* \qquad (8)$$

The correlation coefficients of the Arrhenius plots (r) of the thermal decomposition steps were found to lie in the range 0. 8661 to 0.9968, showing a good fit with linear function. It is clear that the thermal decomposition process of the two complexes is non-spontaneous, i.e., the complexes are thermally stable.

The ^{1}HNMR spectra

The ^{1}HNMR spectrum of $[ZrO(NOR)_2Cl]Cl.15H_2O$ complex (Figure 5) which was carried out in DMSO-d_6 as a solvent is in agreement with the suggested coordination through the carboxylato group (disappearance of the H(COOH) signal in our complex) and three peaks at δ 2.507, 2.502 and 2.496 ppm for Zr(IV) complex characteristic for quaternary nitrogen ($-^+NH_2$).The peak characteristic for water molecules was observed at δ 3.555, 3.429, 3.374 and 3.166 ppm, which weren't found in the free norfloxacin. The ^{1}HNMR data for free NOR and this complex are summarized in Table 5 and all assignments are given [24,26,38].

The sample of UO_2^{2+} complex is rejected when it was sent to make ^{1}HNMR spectrum because I think the uranium metal is a radioactive element and may be radiate a radiation when it is affected by an electromagnetic radiation and this make a corruption to the field of the instrument used Varian Mercury VX-300 NMR Spectrometer [25,27].

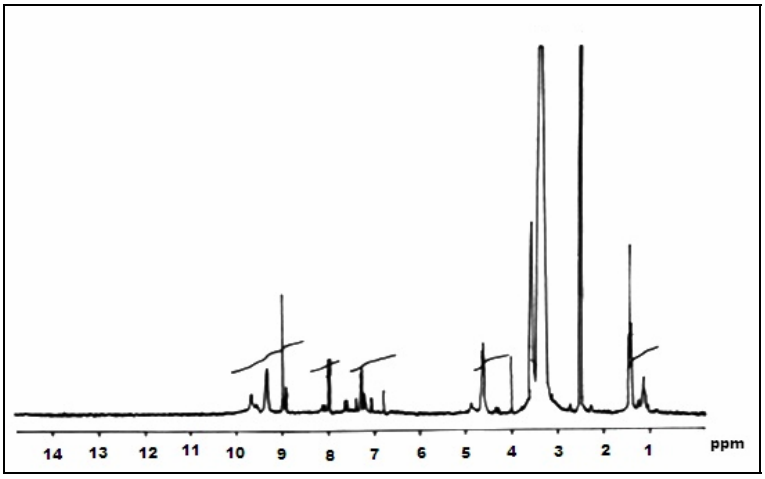

Figure 5. ^{1}HNMR spectrum of $[ZrO(NOR)_2Cl]Cl.15H_2O$ complex in DMSO, δ_{TMS}.

Table 5. ^{1}HNMR values (ppm) and tentative assignments for (A) NOR and (B) $[ZrO(NOR)_2Cl]Cl.15H_2O$ complex.

A	B	Assignments
1.13 [24,26,38]	1.053, 1.119, 1.389, 1.436	δ H, -CH_3
2.0 [24,26,38]	2.496, 2.502, 2.507	δ H, -$^{+}NH_2$
- [24,26,38]	3.166, 3.374, 3.429, 3.555	δ H, H_2O
2.78, 3.10, 3.47 [24,26,38]	4.001, 4.589, 4.612, 4.634	δ H, -CH_2 aliphatic
5.93, 7.12, 8.01 [24,26,38]	7.583, 7.629, 7.957, 8.001	δ H, -CH_2 aromatic
11.00 [24,26,38]	-	δ H, -COOH

Antibacterial investigation

The antibacterial activity of the ligand and their complexes, was studied against three bacterial species, such as *Staphylococcus aureus (S.aureus), Escherichia coli (E.coli)* and *Pseudomonas aeruginosa (P.aeruginosa)* and antifungal screening was studied against two fungi species, *penicillium (P. rotatum)* and *trichoderma (T. sp*.). Screening was performed by determining the inhibition zone diameter values (mm) of the novel investigated compounds against microorganisms and the results obtained are found in Figure 6 in Table 6. A comparative study of ligand and their metal complexes showed that they exhibit higher antibacterial activity than uncomplexed ligand. The results are promising compared with the previous studies [50-52] and no antifungal activity observed for ligand and their complexes. Such increased activity of metal chelate can be explained on the basis of the overtone concept and chelation theory. According to the overtone concept of cell permeability, the lipid membrane that surrounds the cell favors the passage of only lipid-soluble materials in which liposolubility is an important factor that controls the antimicrobial activity. This explain why Gram-negative bacteria (*Escherichia coli (E. coli)* and *Pseudomonas aeruginosa (P. aeruginosa*)) more sensitive than Gram-positive one (*Staphylococcus aureus (S. aureus*)). On chelation the polarity of the metal ion will be reduced to a greater extent due to overlap of ligand orbital and partial sharing of the positive charge of the metal ion with donor groups. Further it increases the delocalization of π-electrons over the whole chelate ring and enhances the lipophilicity of the complexes [51]. This increased lipophilicity enhances the penetration of complexes into the lipid membranes and blocks the metal binding sites in enzymes of microorganisms. These complexes also disturb the respiration process of the cell and thus block the synthesis of proteins, which restricts further growth of the microorganisms.

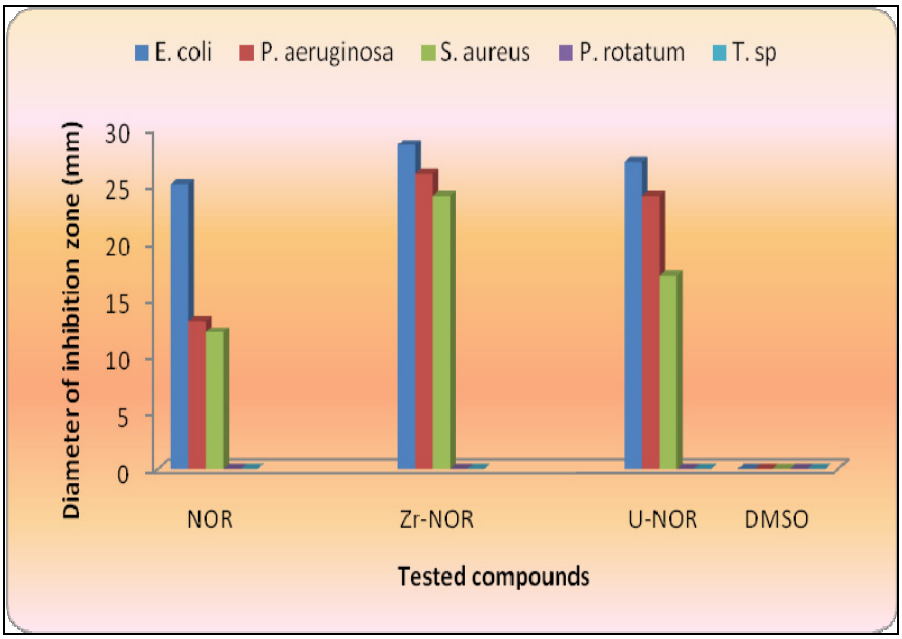

Figure 6. Statistical representation for biological activity of norfloxacin and its complexes.

Table 6. The inhibition diameter zone values (mm) for NOR and its compounds.

Compounds	Microbial species				
	Bacteria			Fungi	
	E. coli	*P. aeruginosa*	*S. aureus*	*P. rotatum*	*T. sp*
NOR	25.0 ±0.881	13.0 ±0.2887	12.0 ±0. 0.839	0	0
$[ZrO(NOR)_2Cl]Cl.15H_2O$	28.5^{+1} ±0.600	26.0^{+3} ±0.9238	24.0^{+2} ±0.635	0	0
$[UO_2(NOR)_3](NO_3)_2.4H_2O$	27.0^{+1} ±0.881	24.0^{+2} ±0.9815	17.0^{+1} ±0.932	0	0
Control (DMSO)	0	0	0	0	0

Statistical significance $^{(NS)}$not significant, P>0.05; $^{(+1)}$significant, P<0.05; $^{(+2)}$highly significant, P <0.01; $^{(+3)}$ very highly significant, P<0.001; student's *t*-test.

Computational details

Computational method

The geometric parameters and energies were computed by density functional theory at the B3LYP/CEP-31G level of theory, using the GAUSSIAN 98W package of the programs, on geometries that were optimized at CEP-31G basis set. The high basis set was chosen to detect the energies at a highly accurate level. The atomic charges were computed using the natural atomic orbital populations. The B3LYP is the key word for the hybrid functional [53], which is a linear combination of the gradient functionals proposed by Becke [54] and Lee, Yang and Parr [55], together with the Hartree-Fock local exchange function [56].

Structural parameters and models

Norfloxacin

The biological activity of quinolones is mainly determined by its fine structure, the norfloxacin has many characteristic structural features. The molecule is a highly sterically-hindered, the piperazine group is out of plane of the molecule. This observation is supported by the values of calculated dihedral angles: C15N14C12C13, -106.19˚, and C19N14C12C13, 104.13˚ while the dihedral angle C19N14C12C11, -75.59˚ where the values are neither zero nor 180˚. Formula III, shows the optimized geometrical structure of norfloxacin molecule, the dihedral angles O21C3C2C1 is 5.01˚ (almost 0.0) and O23C1C2C3 is 12.66˚ (almost 0.0) which confirms a cis configuration of O21 and O23 while O22C1C2C3 is -169.44˚ which indicates that O21 and O23 are in cis configuration and C3O21 in the same plane of C1O23 while, O22 and O21 are in trans configuration and C3O21 not in the same plane of C1O22.

Table 7 gives the optimized geometry of norfloxacin as obtained from B3LYP/CEP-31G calculations. These data are drawing to give the optimized geometry of molecule. The bond distance of C1-O23 is 1.28Å and C1-O22 is 1.30Å while, C3-O21 is 1.27Å. The value of bond angle C3C2C1 is 126.99˚ reflects on sp^2 hybridization of C2, the same result is obtained with C3 and C1. The values of bond distances are compared nicely with that obtained from X-ray data [57].

Charge distribution on the optimized geometry of norfloxacin is given in Table 7. There is a significant built up of charge density on the oxygen atoms which distributed over all molecule so norfloxacin molecule behaves as bi-dentate ligand (O_{keto} and $O_{carboxilic}$ atoms) and the molecule is a highly dipole μ= 42.86.

Zirconium(IV)-norfloxacin complexes

The Zr(IV) may be chelated with two molecules of norfloxacin through four coordinate bonds (O_{keto} and $O_{carboxylic}$ atoms) from each molecule. The experimental data set that the result complex is six-coordinate so the complex consists of four coordinate bonds with two norfloxacin molecules and one coordinated bond may be with water molecule or chloride ion beside oxygen atom of ZrO ion. In this part we study theoretically the all possible structures can be obtained $[ZrO(NOR)_2]^{2+}$, $[ZrO(NOR)_2Cl]^{+}$ and $[ZrO(NOR)_2H_2O]^{2+}$.

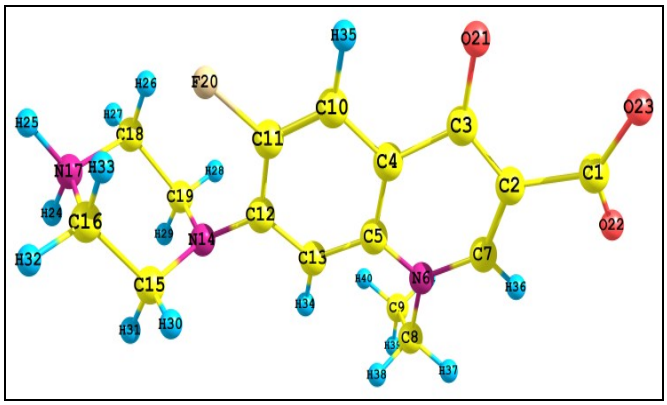

Formula III. The optimized geometrical structure of norfloxacin by using B3LYP/CEP-31G.

Table 7, Equilibrium geometric parameters bond lengths (Å), bond angles (˚), dihedral angles (˚) and charge density of norfloxacin ligand by using DFT/B3LYP/CEP-31G.

Bond length (Å)			
C3-O21	1.27 (1.30) [57]	C1-C2	1.58 (1.47) [57]
C2-C3	1.47 (1.41)	C1-O22	1.30 (1.29)
C2-C7	1.38 (1.38)	C1-O23	1.28 (1.23)
Bond angle (˚)			
C12N14C15	119.86	O21C3C2	128.17
C12N14C19	119.51	O22C1C2	113.13
N14C12C11	122.73	O23C1C2	116.91
N14C12C13	119.79	O23C1O22	129.92
C3C2C1	126.99		
Dihedral angles (˚)			
C16C15N14C12	-95.43	C19N14C12C11	-75.59
C12N14C19C18	95.24	C19N14C12C13	104.13
C15N14C12C11	74.09	O23C1C2C3	12.66
N14C12C11C10	179.98	O22C1C2C3	-169.44
N14C12C13C5	-179.30	O21C3C2C1	5.01
C15N14C12C13	-106.19		
Charges			
N17	0.257	O21	-0.097
N14	-0.117	O22	-0.340
N6	0.213	O23	-0.250
C3	-0.269	C1	-0.141
Total energy/au		-202.66371	
Total dipole moment/D		42.86	

( ): Ref. [57].

Description of the structure of $[ZrO(NOR)_2]^{2+}$

Formula IV shows the optimized geometrical structure of the complex with the atomic numbering scheme selected bond distances and angles are given in Table 8. The suggested complex is composed of $[ZrO(NOR)_2]^{2+}$.

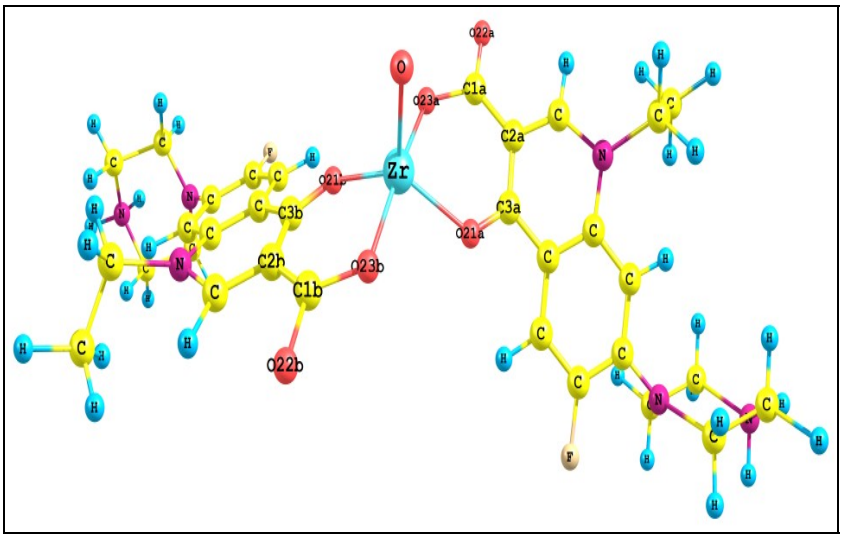

Formula IV. Optimized geometrical structure of $[ZrO(NOR)_2]^{2+}$ complex by using B3LYP/CEP-31G

The zirconium ion in zirconyl complex with coordination number five, at a crystallographic inversion center, is in a structural similar to a square pyramidal environment. In the equatorial plane the metal ion is coordinated by four oxygen atoms (O_{keto} and $O_{carboxylic}$) of two norfloxacin ligands at the distances vary from 1.982Å to 2.104Å, these bond lengths are similar to those observed in related compounds [58,59]. The square pyramidal coordination environment is produced and bond distance between Zr-O23a is 2.104Å [59] and Zr-O21a is 2.091Å [58] while the distance between Zr-O23b is 2.025Å [59] and Zr-O21b is 1.982Å [58]. The bond angles around the central metal ion Zr(IV) vary from 83.41˚ to 115.64˚; these values differ significantly from these expected for a regular a square pyramidal structure.

The distances and angles within the ligand moiety are similar to those described for free norfloxacin [57]. The energy of this complex is -466.40174 au while the dipole moment is weak 3.362D, so this complex is less stable and the band gab between HOMO and LUMO is 0.425 au.

Table 8. Equilibrium geometric parameters bond lengths (Å), bond angles (˚) and charge density of $[ZrO(NOR)_2]^{2+}$ by using DFT/B3LYP/CEP-31G.

Bond length (Å)			
Zr-O21a	2.091 (1.943) [58]	C1b-O22b	1.378
Zr -O23a	2.104 (2.197) [59]	C3b-O21b	1.238
Zr -O21b	1.982 (1.943) [58]	C1a-O23a	1.354
Zr -O23b	2.025 (2.197) [59]	C1a-O22a	1.365
Zr –O	2.021	C3a-O21a	1.265
		C1b-O23b	1.352
Bond angle (˚)			
O21b Zr O23b	88.99 (96.05) [62]	O21a Zr O23b	92.40 (96.50) [62]
O21b Zr O23a	90.11 (96.50) [62]	O21a Zr O	115.64
O21b Zr O	115.52	O23a Zr O	92.41
O21a Zr O23a	83.41		
O23b Zr O	93.59		
Charges			
Zr	0.915	O	0.221
O23a	-0.364	O23b	-0.357
O21a	-0.288	O21b	-0.305
O22a	-0.358		
O22b	-0.347		
Total energy/au		-466.40174	
Total dipole moment/D		3.362	
Energy gab/au		0.425	

Description of the structure of $[ZrO(NOR)_2H_2O]^{2+}$

Table 9 lists selected inter atomic distances and bond angles. The structure of the complex with atomic numbering scheme is shown in Formula V. The complex consists of two units of norfloxacin molecule and one water molecule with metal ion Zr(IV). The complex is six-coordinate with distorted octahedral environment around the metal ion. The metal ion Zr(IV) of ZrO is coordinated to one O_{keto} atom and one $O_{carboxylate}$ atom of norfloxacin ligand and O_{H2O} atom for water. The Zr-O21a and Zr-O21b bond lengths are 2.068Å and 2.066Å, respectively, which are longer than that Zr-O23a and Zr-O23b which found at 2.063Å and 2.167Å, respectively, and the bond distance between Zr-O_{H2O} is 2.114 Å [60]. Also the angles around the central metal ion Zr(IV) with surrounding oxygen atoms vary from 85.08˚ to 95.67˚; these values not differ legally from these expected for a regular octahedron. The distances and angles in the quinolone ring system, as well as those of piprazine rings are similar to those found in reported structure of free norfloxacin and norfloxacin compounds [57]. The energy of this complex is -473.073547 au while the dipole

moment is weak 3.580D, so this complex is less stable and the band gab between HOMO and LUMO is 0.303 au.

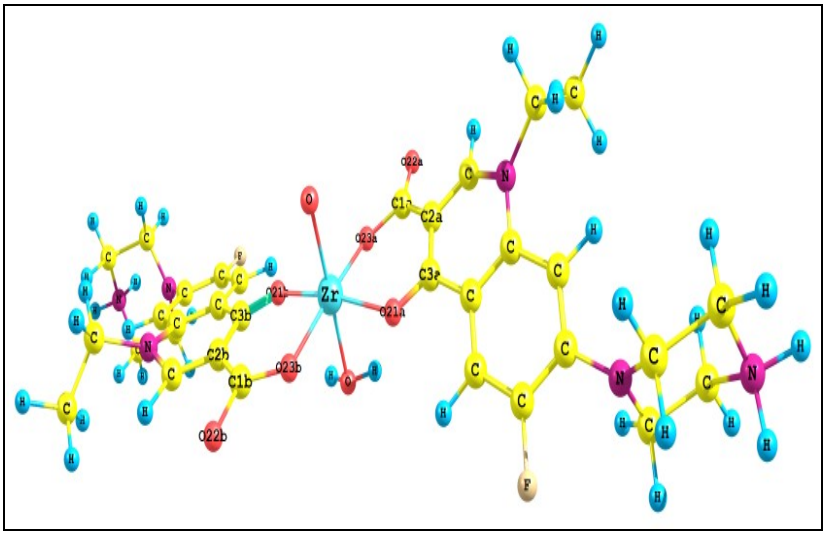

Formula V. Optimized geometrical structure of $[ZrO(NOR)_2(H_2O)]^{2+}$ complex by using B3LYP/CEP-31G.

Description of the structure of $[ZrO(NOR)_2Cl]^+$

Table 10 lists selected inter atomic distances and angles. The structure of the complex with atomic numbering scheme is shown in Formula VI. The complex consists of two units of norfloxacin molecule and one chloride ion with Zr(IV) ion. The complex is six-coordinate with distorted octahedral environment around the metal ion. The Zr(IV) is coordinated to one O_{keto} atom and one $O_{carboxylate}$ atom of norfloxacin ligand and Cl ion. The Zr-O21a and Zr-O21b bond lengths are 2.067Å and 2.064Å, respectively, which are longer than that Zr-O23a and Zr-O23b which found at 2.063Å and 2.161Å, respectively, and the bond distance between Zr-Cl is 2.446 Å [61]. Also the angles around the central metal ion Zr(IV) with surrounding oxygen atoms vary from 85.59˚ to 92.25˚; these values agree quite well with these expected for distorted octahedron. The distances and angles in the quinolone ring system, as well as those of piprazine rings are similar to those found in reported structure of free norfloxacin and norfloxacin compounds [57].

The bond distances between Zr(IV) and surrounded oxygen atoms of norfloxacin in water complex are larger than that in chloride complex as shown in Tables 9 and 10, so that the metal ion Zr(IV) is bonded strongly with surrounded oxygen atoms of norfloxacin in chloride complex more than that in water complex. Also the charge accumulated on $O_{carboxylate}$ (-0.313 and -0.318) and O_{keto} (-0.292 and -0.331), in water complex while, $O_{carboxylate}$ (-0.352 and -0.331) and O_{keto} (-0.302 and -0.338), in chloride complex. There is a strong interaction between central metal ion Zr(IV) which become has charge equal +0.971. The energy of this complex is more negative than other complexes -481.844 au and highly dipole 5.34D. For all these reasons the chloride complex is more stable than other complexes and Zr(IV) favor coordinated with one ion of chloride more than one molecule of water to complete the octahedron structure. The energy barrier of this complex is the band gab between HOMO and LUMO is 0.131 au, the lower value of band gab corresponding with

larger wave length so the chloride complex expected to be more dens colored and conjugate, these results corresponding to larger value of dipole moment.

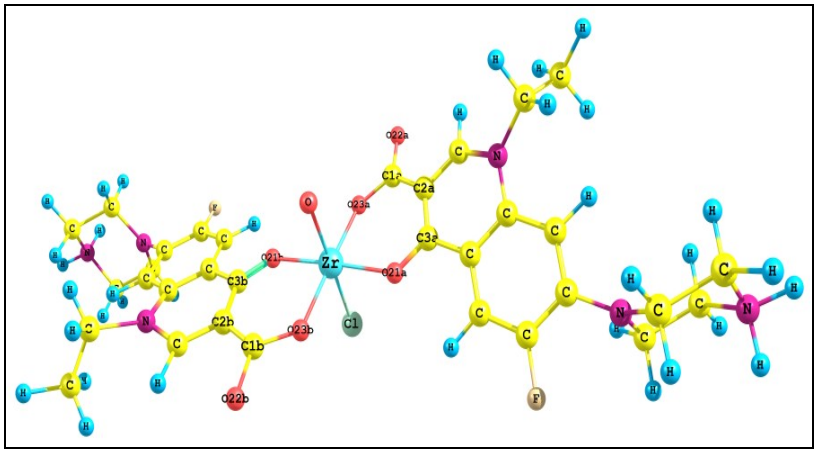

Formula VI. Optimized geometrical structure of $[ZrO(NOR)_2Cl]^+$ complex by using B3LYP/CEP-31G.

Uranium(VI)-norfloxacin complex

Uranyl models were not included in this work because Uranium atom has large number of electrons, so the atomic number of uranium atom out of the range of CEP-31G basic set. The relativistic effects of uranium atom were considered using Relativistic Effective Core Potentials (RECPs), which also replaced the Core electrons. We didn't use this method of calculation before so we try to know how this method of calculation proceeds.

Conclusions

Two new Zr(IV) and U(VI) complexes with norfloxacin (NOR) in methanol and acetone, at room temperature have been synthesized. Elemental analysis, IR, UV-VIS., ^{1}HNMR, conductance measurements and thermogravimetric analysis (TG) and differential thermal analysis (DrTGA) have been used to characterize the isolated solid complexes. The kinetic parameters of thermogravimetric (TG) and its differential (DrTGA), such as entropy of activation, pre-exponential factors, activation energy evaluated by using Coats-Redfern and Horowitz-Metzger equations. The exact structure of Zr(IV) complex was detected by using the density functional theory (DFT). Antimicrobial studies were carried out against several bacterial species and antifungal. The results showed significant increase in antibacterial activity of metal complexes as compared with uncomplexed ligand and no antifungal activity observed for ligand and their complexes.

Table 9. Equilibrium geometric parameters bond lengths (Å), bond angles (˚) and charge density of $[ZrO(NOR)_2(H_2O)]^{2+}$ by using DFT/B3LYP/CEP-31G.

Bond length (Å)			
Zr-O21a	2.068 (1.943) [58]	C1b-O22b	1.363
Zr-O23a	2.063 (2.197) [59]	C3b-O21b	1.212
Zr-O21b	2.066 (1.943) [58]	C1a-O23a	1.355
Zr-O23b	2.167 (2.197) [59]	C1a-O22a	1.363
Zr-O	2.012	C3a-O21a	1.264
Zr-O_{H2O}	2.114	C1b-O23b	1.354
Bond angle (˚)			
O21bZrO23b	86.48 (72.64) [62]	O21aZrO23b	94.43
O21bZrO23a	93.14 (96.05) [62]	O21aZrO	95.67
O21bZrO	94.49	O21aZrO_{H2O}	84.78
O21bZrO_{H2O}	85.08	O23aZrO	92.47
O21aZrO23a	85.18	O23aZrO_{H2O}	88.31
O23bZrO	91.91	O23bZrO_{H2O}	87.32
Charges			
Zr	0.832	O	0.157
O23a	-0.313	O_{H2O}	-0.298
O21a	-0.292	O23b	-0.318
O22a	-0.317	O21b	-0.331
O22b	-0.368		
Total energy/au		-473.073547	
Total dipole moment/D		3.580	
Energy gab/au		0.303	

Table 10. Equilibrium geometric parameters bond lengths (Å), bond angles (˚) and charge density of $[ZrO(NOR)_2Cl]^+$ by using DFT/B3LYP/CEP-31G.

Bond length (Å)			
Zr-O21a	2.067 (1.943) [58]	C1b-O22b	1.363
Zr-O23a	2.063 (2.197) [59]	C3b-O21b	1.212
Zr-O21b	2.064 (1.943) [58]	C1a-O23a	1.354
Zr-O23b	2.161 (2.197) [59]	C1a-O22a	1.363
Zr-O	2.012	C3a-O21a	1.263
Zr-Cl	2.446 (2.437) [59] (2.482) [58]	C1b-O23b	1.353
Bond angle (˚)			
O21bZrO23b	86.54 (72.64) [62]	O21aZrO23b	91.89
O21bZrO23a	90.03 (96.05) [61]	O21aZrO	92.25
O21bZrO	90.24	O21aZrCl	88.90
O21bZrCl	88.60	O23aZrO	90.26
O21aZrO23a	85.59	O23aZrCl	90.22
O23bZrO	88.84	O23bZrCl	90.72
Charges			
Zr	0.970	O	0.202
O23a	-0.352	Cl	-0.325
O21a	-0.302	O23b	-0.331
O22a	-0.284	O21b	-0.338
O22b	-0.344		
Total energy/au		-481.843559	
Total dipole moment/D		5.340	
Energy gab/au		0.131	

References

[1] H. Koga, A. Itoh, S. Murayama, T. Irikura, *J. Med. Chem.*, **1980**, *23*, 1358.

[2] G.Y. Lesher, E.J. Froelich, M.D. Gruett, J.H. Bailey, R.P. Brundage, *J. Pharm.Chem*., **1962**, *5*, 1063.

[3] B.M. Lomaestro, G.R. Bailie, *Ann-Pharmacother*., **1991**, *25*, 1249.

[4] N.C. Baenziger, *Acta Crystallogr.*, **1986**, *C 42*, 1505.

[5] C. Chulvi, M.C. Muñoz, L. Perellò, R. Ortiz, M.I. Arriortua, J. Via, K. Urtiaga, J.M. Amigò, L.E. Ochando, *J. Inorg. Biochem*., **1991**, *42*, 133.

[6] I. Turel, I. Leban, N. Bukovec, *J. Inorg. Biochem.*, **1994**, *56*, 273.

[7] M. Ruiz, L. Perellò, R. Ortiz, A. Castiñeiras, C. Maichle-Mössser, E. Cantòn, *J. Inorg. Biochem*., **1995**, *59,* 801.

[8] M. Ruiz, L. Perello, J. Servercarrio, R. Ortiz, S. Garciagranda, M.R. Diaz, E. Canton, *J. Inorg. Biochem*., **1998**, *69*, 231.

[9] G.M. Diaz, L.M.R. Martinez-Aquilera, R.P. Alfonso, *Inorg. Chim. Acta*, **1987**, *138*, 41.

[10] G.M.Diaz, L.M.R. Martinez-Aquilera, R. Moreno-Esparza, K.H. Pannell, F. Cervantes-Lee, J. *Inorg. Biochem.*, *1993*, *50*, 65.

[11] M. Ruiz, R. Ortiz, L.Perello, *Inorg. Chim. Acta*, **1993**, *211*,133.

[12] M. Ruiz, R. Ortiz, L.Perello, *Inorg. Chim. Acta*, **1994**, *217*, 149.

[13] S.C. Wallis, L.R. Gahan, B.G. Charles, T.W. Hambley, *Polyhedron*, **1995**, *14*, 2835.

[14] S.C. Wallis, L.R. Gahan, B.G. Charles, T.W. Hambley, P.A. Duckworth, *J. Inorg. Biochem*., **1996**, *62*, 1.

[15] I. Turel, I. Leban, P. Bukovec, M. Barbo, *Acta Cryatallogr.*, **1997**, *C 53*, 942.

[16] Gaussian 98, Revision A.6, M.J. Frisch, G.W. Trucks, H.B. Schlegel, G.E. Scuseria, M.A. Robb, J.R. Cheeseman, V.G. Zakrzewski, J.A. Montgomery, Jr., R.E. Stratmann, J.C. Burant, S. Dapprich, J.M. Millam, A.D. Daniels, K.N. Kudin, M.C. Strain, O. Farkas, J. Tomasi, V. Barone, M. Cossi, R. Cammi, B. Mennucci, C. Pomelli, C. Adamo, S. Clifford, J. Ochterski, G.A. Petersson, P.Y. Ayala, Q. Cui, K. Morokuma, D.K. Malick, A.D. Rabuck, K. Raghavachari, J.B. Foresman, J.Cioslowski, J.V. Ortiz, B.B. Stefanov, G. Liu, A. Liashenko, P. Piskorz, I. Komaromi, R. Gomperts, R.L. Martin, D.J. Fox, T. Keith, M.A. Al-Laham, C.Y. Peng, A. Nanayakkara, C. Gonzalez, M. Challacombe, P.M.W. Gill, B. Johnson, W. Chen, M.W. Wong, J.L. Andres, C. Gonzalez, M. Head-Gordon, E.S. Replogle, J.A. Pople, Gaussian, Inc., Pittsburgh PA, 1998.

[17] W.J. Stevens, M. Krauss, H. Bosch, P.G. Jasien, *Can. J. Chem*., **1992**, *70*, 612.

[18] V. Alexeyev, *Quantatitative analysis*, 2nd ed., Indian, 1969, pp.406.

[19] D.J. Beecher, A.C. Wong, *Appl. Environ. Microbial*., **1994**, *60*, 1646.

[20] W.J.Geary, *Coord. Chem. Rev*., **1971**, *7*, 81.

[21] R.M. Silverstein, G.C. Bassler, T.C. Morril, *Spectroscopic Identification of Organic Compounds,* 5th ed., Wiley, New York, 1991.

[22] J. Al-Mustafa; *Acta Chim. Slov*., **2002**, *49*, 457.

[23] S.A. Sadeek, *J. Mol. Struct.*, **2005**, *753*, 1.

[24] S.A. Sadeek, M.S. Refat, H.A. Hashem, *J. Coord. Chem*., **2006**, *59*, 7.

[25] S.A. Sadeek, W.H. EL-Shwiniy, *J. Mol. Struct*., **2010**, *977*, 243.

[26] S.A. Sadeek, W.H. EL-Shwiniy, W.A. Zordok, A.M. EL-Didamony, *J. Argent. Chem. Soc*., in press, **2010.**

[27] S.A. Sadeek, W.H. EL-Shwiniy, *J. Coord. Chem*., in press, **2010**.

[28] N. Sultana, A. Naz, M.S. Arayne, M.A. Mesaik, *J. Mol. Struct.*, **2010**, *969*, 17.

[29] E.K. Efthimiadou, A. Karaliota, G. Pasomas, *J. Inorg. Biochem*., **2010**, *104*, 455.

[30] I. Turel, L. Leban, G. Klintschar, N. Bukovec, S. Zalar, *J. Inorg. Biochem*., **1997**, *66*, 77.

[31] I. Turel, L. Leban, N. Bukovoec, *J. Inorg. Biochem*., **1997**, *66*, 241.

[32] K. Nakamoto, *Infrared and Raman Spectra of Inorganic and Coordination Compounds*, 4th ed., Wiley, New York, 1986, PP. 230.

[33] G.B. Deacon, R.J. Phillips, *Coord. Chem. Rev*., **1980**, *33*, 227.

[34] Z.F. Chen, R.J. Xiong, J.L. Zuo, Z. Guo, X.Z. You, K.H. Fun, *J. Chem. Soc., Dalton Trans*., **2000**, *22*, 4013.

[35] S.P. Mcglynnm, J.K. Smith, W.C. Neely, *J. Chem. Phys.*, **1961**, *35*, 105.

[36] L.H. Jones, *Spectrochim. Acta*, **1959**, *15*, 409.

[37] S.A. Sadeek, S.M. Teleb, M.S. Refat, M.A.F. Elmosallamy, *J. Coord. Chem*., **2005**, 58, 1077.

[38] M.S. Refat, *Spectrochim. Acta*, **2007**, *68*, 1393.

[39] F.A. Cotton, G. Wilkinson, C.A. Murillo, M. Bochmann, *Advanced Inorganic Chemistry*, 6th ed., Wiley, New York, 1999, PP. 857.

[40] F.A. Cotton, C.W. Wilkinson, *Advanced Inorganic Chemistry*, 3rd ed., Interscience publisher, New York, 1972.

[41] E.S. Freeman, B. Carroll, *J. Phys. Chem*., **1958**, *62*, 394.

[42] J. Sestak, V. Satava, W.W. Wendlandt, *Thermochim. Acta*, **1973**, *7*, 333.

[43] A.W. Coats, J.P. Redfern, *Nature*, **1964**, *201*, 68.

[44] T. Ozawa, *Bull. Chem. Sot. Jpn.*, **1965**, *38*, 1881.

[45] W W. Wendlandt, *Thermal methods of analysis*, Wiley, New York, 1974.

[46] H.W. Horowitz, G. Metzger, *Anal. Chem*., **1963**, *35*, 1464.

[47] J.H. Flynn, L.A. Wall, *Polym. Lett.*, **1966**, *4*, 323.

[48] P. Kofstad, *Nature*, **1957**, *179*, 1362.

[49] J.H. Flynn, L.A. Wall, *J. Res. Natl. Bur. Stand*., **1996**, *70 A*, 487.

[50] M.N. Hughes, *The Inorganic Chemistry of Biological Processes*, 2nd ed., Wiley, New York, 1981.

[51] M. Imran, J. Iqbal, S. Iqbal, N. Ijaz, *Turk, J. Biol.*, **2007**, *31*, 67.

[52] E.K. Efthimiadou, A. Karaliota, G. Pasomas, *J. Inorg. Biochem.*, **2010**, *104*, 455.

[53] W. Kohn, L.J. Sham, *Phys. Rev A*, **1965**, *140*, 1133.

[54] A.D. Becke, *Phys. Rev. A*, *1988*, *38*, 3098.

[55] C. Lee, W. Yang, R.G. Parr, *Phys. Rev B*, **1988**, 37.

[56] R.L. Flurry Jr., *Molecular Orbital Theory of Bonding in Organic Molecules*, Marcel Dekker, New York, 1968.

[57] I. Turel, L. Golic, P. Bukovec, M. Gubina, *J. Inorg. Biochem*., **1998**, *71*, 53.

[58] T. Cuenca, P. Gomez-Sal, C. Martin, B. Royo, P. Royo, *J. Organomet.Chem*., **1999**, *588*, 134.

[59] D.P. Steinhuebel, P. Fuhrmann, S.J. Lippard, *Inorg. Chem. Acta*, **1998**, *270*, 527.

[60] G. Paolucci, M. Vignola, L. Coletto, B. Pitteri, F. Benetollo, *J. Organomet. Chem*., **2003**, *687*, 161.

[61] A. Antinolo, R. Fernandez-Galan, A. Otero, S. Prashar, I. Rivilla, A.M. Rodriguez, *J. Organomet. Chem*., **2006**, *691*, 2924.

[62] W. Petz, F. Weller, E.V. Avtomonov, *J. Organomet. Chem*., **2000**, *598*, 403.